Published in final edited form as:
*Free Radic Biol Med*. 2013 December ; 65: . doi:10.1016/j.freeradbiomed.2013.06.042.

# Folic Acid Reverses Nitric Oxide Synthase Uncoupling and Prevents Cardiac Dysfunction in Insulin Resistance: Role of $Ca^{2+}$/Calmodulin-Activated Protein Kinase II

**Nathan D. Roe**[1], **Emily Y. He**[1,2], **Zhenbiao Wu**[2], and **Jun Ren**[1]

[1]Center for Cardiovascular Research and Alternative Medicine, University of Wyoming, Laramie, WY 82071, USA

[2]Department of Clinical Immunology, Xijing Hospital, the Fourth Military Medical University, Xi'an, China 710032

## Abstract

Nitric oxide synthase (NOS) may be uncoupled to produce superoxide rather than nitric oxide (NO) under pathological conditions such as diabetes mellitus and insulin resistance, leading to cardiac contractile anomalies. Nonetheless, the role of NOS uncoupling in insulin resistance-induced cardiac dysfunction remains elusive. Given that folic acid may produce beneficial effect for cardiac insufficiency partially through its NOS recoupling capacity, this study was designed to evaluate the effect of folic acid on insulin resistance-induced cardiac contractile dysfunction in a sucrose-induced insulin resistance model. Mice were fed a sucrose or starch diet for 8 weeks prior to administration of folic acid in drinking water for an additional 4 weeks. Cardiomyocyte contractile and $Ca^{2+}$ transient properties were evaluated while myocardial function was assessed using echocardiography. Our results revealed whole body insulin resistance following sucrose feeding associated with diminished NO production, elevated peroxynitrite ($ONOO^-$) levels, as well as impaired echocardiographic and cardiomyocyte function along with a leaky ryanodine receptor (RYR) and intracellular $Ca^{2+}$ handling derangement. Western blot analysis depicted that insulin resistance significantly promoted $Ca^{2+}$/Calmodulin-dependent protein kinase II (CaMKII) phosphorylation which might be responsible for the leaky RYR and cardiac mechanical dysfunction. NOS recoupling using folic acid reversed insulin resistance-induced changes in NO and $ONOO^-$, CaMKII phosphorylation and cardiac mechanical abnormalities. Taken together, these data demonstrated that treatment with folic acid may reverse cardiac contractile and intracellular $Ca^{2+}$ anomalies through ablation of CaMKII phosphorylation and RYR $Ca^{2+}$ leak.

### Keywords

Insulin resistance; folic acid; cardiac function; intracellular $Ca^{2+}$; CaMKII



Correspondence should be addressed to: Dr. Jun Ren, University of Wyoming College of Health Sciences, Laramie, WY 82071, USA. Tel : (307) 766-6131; Fax: (307) 766-2953; jren@uwyo.edu.



**DISCLOSURES:** None

## INTRODUCTION

Type 2 diabetes mellitus is a significant health problem in the United States and continues to rise with the prevalence of obesity. Cardiovascular diseases are the leading cause of death among diabetic individuals but available treatments are limited to symptom control of cardiovascular problems [1]. One of the early indicators of diabetes development is impaired ability to respond to insulin, termed insulin resistance. During insulin resistance prior to the onset of diabetes, the accumulation of reactive oxygen species (ROS) can be seen in hearts [2], which contributes to cardiac dysfunction through peroxidation of lipids and proteins, extracellular matrix remodeling, mitochondrial damage, and alteration in the excitation contraction coupling proteins [3]. Several sources of ROS have been identified in the heart under insulin resistance including nicotinamide adenine dinucleotide phosphate (NADPH) oxidase, xanthine oxidase, mitochondria, and uncoupled nitric oxide synthase (NOS) [3]. Recent evidence has depicted a pivotal pathological role of uncoupled NOS as a primary source in the heart while drug therapy targeting this enzyme has shown some promises in the management of heart diseases [4–6].

Folic acid has been shown to exhibit beneficial effects in a wide array of heart diseases. During ischemia reperfusion, high dose folic acid may prevent myocardial dysfunction, preserve high energy phosphate, abrogate ROS generation and eNOS uncoupling [7]. In the vasculature, folic acid treatment may reduce abdominal aortic aneurysm formation and prevent eNOS uncoupling, which may be associated with its stimulatory effect on dihydrofolate reductase [8, 9]. Hyperhomocysteinemia is an important independent risk factor for cardiovascular diseases. It has been suggested that the detrimental effect of homocysteine can be alleviated by folic acid administration with a concurrent reduction of superoxide generation [10, 11]. Previous evidence has implicated the therapeutic potential of folic acid in cardiovascular disorders in particular NOS uncoupling [12] although the impact of folic acid on insulin resistance-induced cardiac complication still remains elusive.

Excitation-contraction coupling in the heart involves three types of $Ca^{2+}$ channel in particular L-type $Ca^{2+}$ channel, ryanodine receptor (RYR), $Na^{+}$-$Ca^{2+}$ exchanger and sarco(endo)plasmic reticulum $Ca^{2+}$-ATPase (SERCA) [13]. Among which, RYR is responsible for $Ca^{2+}$-induced $Ca^{2+}$ release to initiate myocardial contraction. RYR is susceptible to posttranslational modification by oxidation or phosphorylation leading to $Ca^{2+}$ leak *en route* to onset and development of arrhythmic and myopathic alterations [14]. A number of signaling machineries have been put forward for the regulation of RYR. $Ca^{2+}$/Calmodulin-dependent protein kinase II (CaMKII) is a protein the activation of which leads to phosphorylation of RYR, subsequently $Ca^{2+}$ leak and contractile aberration [15]. Although a detrimental role of CaMKII phosphorylation has been reported is identified in diabetes [16], little is known for CaMKII phosphorylation in the setting of insulin resistance. To this end, the aim of this study was to evaluate if cardiac dysfunction in the setting of insulin resistance induced by a high sucrose diet may be reversed with folic acid. In an effort to understand the mechanism behind folic acid-induced response in insulin resistance, a number of cell mechanisms were evaluated in sucrose-fed mouse hearts treated with or with folic acid including NOS uncoupling, levels of NO and peroxynitrite ($ONOO^{-}$), a reactive product of NO and superoxide anion ($O_2^{-}$) [17], RYR function, CaMKII phosphorylation and intracellular $Ca^{2+}$ regulatory proteins.

# MATERIALS AND METHODS

## Experimental animals, intraperitoneal glucose tolerance test (IPGTT) and echocardiographic analysis

Experimental procedures used in this study were approved by the University of Wyoming Institutional Animal Use and Care Committee (Laramie, WY). Insulin resistance was induced in Friend Virus B (FVB) mice as previously described [18]. Briefly, 3 month-old adult FVB mice were randomly divided into two groups to receive either a high starch diet (68% of energy from starch, Research Diets, D11724, New Brunswick, NJ) or a high sucrose diet (68% of energy from sucrose, Research Diets, D11725). After 8 weeks of starch and sucrose feeding, cohorts of mice received folic acid (15 mg/kg/day) or vehicle in drinking water for an additional 4 weeks [8, 9]. Water consumption was monitored to ensure equal dose for all 4 groups. On the last day (23:00 hour) of folic acid treatment, food was removed and all mice were fasted for 12 hours overnight prior to IPGTT the next day [18]. After obtaining a baseline glucose reading, mice were challenged with glucose (2 g/kg, i.p.) and glucose measurements were taken 15, 30, 60 and 120 min after injection. Glucose concentration was assessed using an ACCU-CHEK advantage glucose analyzer (Roche Diagnostics, Indianapolis, IN). Mice were then provided respective starch or sucrose diet following IPGTT with regular drinking water. Cardiac function was assessed the next morning (08:00 hour) using 2-D guided M-mode echocardiography (Sonos 5500) equipped with a 15-6 MHz linear transducer (Phillips Medical Systems, Andover, MD) in anesthetized (Avertin 2.5%, 10 μl/g, i.p.) mice. Fractional shortening was calculated from left ventricular end-diastolic diameter (LVEDD) and left ventricular end-systolic diameter (LVESD) using the following equation (LVEDD-LVESD)/LVEDD. Thirty-six hrs following completion of folic acid treatment (11:00 hour on the next day following echocardiographic assessment), mice were anesthetized with ketamine (80 mg/kg, i.p.) and xylazine (12 mg/kg, i.p.) and sacrificed using cardioectomy to collect heart tissues.

## Cardiomyocyte isolation and cell mechanics

Hearts were removed rapidly from mice sedated with ketamine (80 mg/kg, i.p.) and xylazine (12 mg/kg, i.p.) and perfused with Krebs-Henseleit bicarbonate solution consisting of (in mM) 118 NaCl, 4.7KCl, 1.2 $MgSO_4$, 1.2 $KH_2PO_4$, 25 $NaHCO_3$, 10 HEPES and 11.1 glucose. Hearts were digested with Liberase Blendzyme 4 (Roche Diagnostics) for 15 min. After removal and mincing of left ventricle, $Ca^{2+}$ was added back to a final concentration of 1.25 mM. Cardiomyocytes with no spontaneous contractions and clear edges were used for shortening and $Ca^{2+}$ cycling experiments. IonOptix™ softedge system (IonOptix, Milton MA) was used to assess the mechanical properties of isolated myocytes. Myocytes were mounted on the stage of an Olympus IX-70 microscope in contraction buffer containing (in mM) 131 NaCl, 4 KCl, $1CaCl_2$, 1 $MgCl_2$, 10 glucose and 10 HEPES. Myocytes were stimulated at 0.5 Hz with cell shortening and relengthening evaluated using the indices: peak shortening (PS), time to peak shortening (TPS), time to 90% relengthening ($TR_{90}$) and maximal velocities of shortening/relengthening (± dL/dt).

## Intracellular $Ca^{2+}$ transient, RYR leak and spontaneous contractions

Myocytes were loaded with fura-2/AM (0.5 μM) for 10 min. After washing with contraction buffer (recipe above), fluorescence intensity was recorded with a dual excitation fluorescence photomultiplier system (IonOptix). Myocytes were stimulated at 0.5 Hz and excited at 360 and 380nm with fluorescence emissions detected at 480 and 520 nm, respectively. Intracellular $Ca^{2+}$ levels were calculated using the ratio of the two wavelengths (360/380). Leak from ryanodine receptor was assessed as previously described with minor modification [19, 20]. Myocytes loaded with fura 2/AM were incubated with $0Na^+$ $OCa^{2+}$ buffer containing (in mM) 140 LiCl, 4 KCl, 1 MgCl, 10 glucose, and 5 HEPES with the pH

adjusted to 7.4 using LiOH. Myocytes in $0Na^+$ $0Ca^{2+}$ buffer were mounted on the microscope and intracellular $Ca^{2+}$ levels were assessed for 80 seconds without field stimulation. $0Na^+$-$0Ca^{2+}$ buffer with tetracaine (1 mM) was added and resting $Ca^{2+}$ levels were assessed again. RYR leak was calculated using the area between resting curve and tetracaine curve, [($0Na^+$-$0Ca^{2+}$ AUC) − ($0Na^+$-$0Ca^{2+}$ + tetracaine AUC)]. An Ionwizard analysis software (IonOptix) was used to perform the calculation.

### Superoxide anion production and NOS uncoupling

Superoxide production was assessed as described [20]. In brief, 30 μm tissue sections were cut from fresh unfixed heart sections frozen in O.C.T. (Tissue-Tek, Torrence, CA). Sections were incubated with the non-specific NOS inhibitor Nω-nitro-L-arginine methyl ester (L-NAME, 1 mM) or PBS for 30 min at room temperature prior to incubation with a superoxide specific dye dihydroethidium (DHE, 3 μM, Molecular Probes, Eugene OR) for 30 minutes at room temperature. After washing twice with PBS, tissues were lightly fixed in 2% paraformaldehyde and mounted with Prolong gold antifade (Invitrogen, Calsbad CA). Multiple images per section were acquired using a Zeiss 710 laser scanning confocal microscope. Fluorescence intensity per nucleus was calculated using Image J analysis software (NIH, Bethesda MD). NOS dependent superoxide was calculated by the difference in fluorescence intensity between sections incubated in PBS and those incubated with L-NAME.

### Determination of NO and $ONOO^-$

NO levels were determined colorimetrically after mixing 0.5 ml isolated cardiomyocyte cell lysates and Griess reagent [0.1% N-(1-naphthyl)ethylenediamine in water and 1% sulfanilamide in 5% phosphoric acid]. Concentrations of nitrite were estimated by comparing absorbance readings at 550 nm against standard solutions of $NaNO_2$. $NO_2$-free $H_2O$ was used as negative control [21]. Nitrotyrosine content, a footprint of *in vivo* $ONOO^-$ formation, was determined in myocardial tissues using ELISA. Myocardial tissue was homogenized in ice-cold PBS (1/10 w/v) using a PRO 200 homogenizer followed by sonication with a dismembrator (Fisher Scientific, Pittsburgh, PA). Homogenates were centrifuged for 10 min at 12,500 × *g* at 4°C. Supernatants were collected and samples (50 μg protein) were applied to disposable sterile enzyme-linked immunosorbent assay plates (Corning Glassworks, Corning, NY) prior to overnight incubation at 4°C. The plate was then washed with 200 μl of PBS/0.1% Tween buffer, followed by incubation with heat-inactivated 10% goat serum in PBS for 1 hr at 37°C to block nonspecific binding. The primary antibody (mouse monoclonal antibody against nitrotyrosine from Alexis Biochemicals, San Diego, CA; 1:2000) and secondary antibody (horseradish peroxidase-conjugated anti-mouse IgG, 1:2000) were added, and the peroxidase reaction product was generated using 2.2 mM *O*-phenylenediamine dihydrochloride solution (Abbott Diagnostics, Abbott Park, IL). Plates were incubated for 20 min in the dark at room temperature and reaction was stopped by addition of 50 μl of 1 N HCl. Optical density was measured at 450 nm with a Spectra Max 190 Microplate Spectrophotometer (Molecular Devices, Sunnyvale, CA) [22].

### Western blot analysis

Heart tissue was homogenized in a RIPA lysis buffer and centrifuged at 4°C for 20 min at 12,000xg. Supernatants were removed and protein concentration was measured using the Bradford assay. Samples of equivalent protein concentrations were separated on a 7%, 10%, or 15% SDS-PAGE gel in a mini gel apparatus (Mini-PROTEAN II, Bio-Rad). Membranes were blocked with 5% milk in TBS-Tween20 and incubated in anti-pCaMKII ($Thr^{286}$), anti-CaMKII, anti-GAPDH, anti-α-tubulin (Cell Signaling Technology, Beverly, MA), anti-

OxCaMKII (Met$^{281–282}$) (Millipore, Billerica MA), anti-phospholamban (PLB, Abcam, Cambridge MA), anti-phosphorylated PLB (Ser$^{16}$) (Upstate, Lake Placid NY), and anti-SERCA2a (Pierce, Rockford, IL) antibodies overnight at 4°C. Membranes were rinsed and incubated with horseradish peroxidase (HRP) conjugated secondary antibodies and exposed using enzymatic chemiluminescence.

### Statistical analysis

Data were presented as mean ± SEM. The one-way ANOVA followed by a Tukey's *post hoc* analysis was used to determine statistical significance in most cases. A two-way ANOVA was employed to determine significance for glucose tolerance curve and a two tailed student's t-test was used for comparison of glucose tolerance AUC.

## RESULTS

### Effect of sucrose feeding on biometric parameters, glucose tolerance and heart function

Glucose tolerance test was used to confirm insulin resistance and echocardiography was used to determine cardiac dysfunction after 8 weeks of sucrose feeding. Glucose tolerance test showed that sucrose fed mice exhibited around a 2-fold increase in blood glucose levels at 30, 60, and 120 min after IPGTT challenge. Analysis of the area under the curve (AUC) showed that sucrose fed mice exhibit a significant increase compared to control (Fig. S1). Echocardiographic analysis revealed that sucrose diet feeding suppressed fractional shortening confirming the existence of cardiac dysfunction (Fig. 1). Once insulin resistance and cardiac dysfunction were confirmed, mice were given folic acid in drinking water for 4 more weeks. Biometric analysis revealed that neither sucrose feeding nor folic acid, or a combination of the two, exhibited any effect on organ weights (Table 1). Echocardiographic analysis shows a progressive decrease in cardiac performance after 12 weeks of sucrose feeding compared with that at 8 weeks. Interestingly, folic acid not only prevented progression of this cardiac pathological change but also completely reversed depressed fractional shortening which was present at 8 weeks (Fig. 1).

### Effect of folic acid on insulin resistance-induced cardiomyocyte dysfunction

Analysis of cardiomyocytes revealed insulin resistance induced a significant decrease in cell length, peak shortening (PS), and velocities of shortening and relengthening (± dL/dt). Treatment with folic acid was sufficient to restore PS and ± dL/dt back to control levels without affecting the decrease in cell size (Fig. 2). Intracellular $Ca^{2+}$ transient analysis showed that insulin resistance induced a significant decrease in intracellular $Ca^{2+}$ rise (ΔFFI) while prolonging $Ca^{2+}$ clearance. Folic acid was sufficient to restore intracellular $Ca^{2+}$ rise and $Ca^{2+}$ clearance rate back to control levels (Fig. 3).

### Effect of folic acid on insulin resistance-induced superoxide production, NOS uncoupling, NO and $ONOO^{-}$ generation

Excessive superoxide production leads to deleterious effects on heart function. To this end, levels of superoxide were monitored in cardiac tissue sections to examine NOS uncoupling as a possible source for superoxide. Our data revealed that insulin resistance triggered a significant increase in superoxide levels as indicated by enhanced nuclear DHE fluorescence. To determine if NOS uncoupling contributed to enhanced superoxide production, sections were incubated with L-NAME prior to DHE staining. Our data depicted that the ncreased fluorescence under insulin resistance was restored to control levels when incubated with L-NAME. L-NAME had no significant effect itself. Consistent with increased levels of superoxide (total and L-NAME-dependent), cardiomyocyte NO levels and myocardial ONOO-content (as measured by nitrotyrosine formation) were significantly

decreased and increased, respectively, in insulin resistance. Although folic acid did not affect levels of superoxide (total and L-NAME-dependent), NO and ONOO-by itself, it abrogated insulin resistance-induced changes in superoxide, NO and $ONOO^-$ (Fig. 4).

### Insulin resistance induced changes in RYR2

To examine the effect insulin resistance on myocardial intracellular $Ca^{2+}$ cycling, we examined intracellular $Ca^{2+}$ leak from the RYR2 $Ca^{2+}$ channel. Cardiomyocytes from insulin resistant mice exhibited an increase in tetracaine-sensitive intracellular $Ca^{2+}$ rise, indicating the nature of RYR as an origin for $Ca^{2+}$ release. Interestingly, cardiomyocytes from insulin resistant mice receiving folic acid displayed a much smaller RYR2-dependent intracellular $Ca^{2+}$ rise resembling the magnitude of control group. Such rise in intracellular $Ca^{2+}$ under insulin resistance was associated with spontaneous $Ca^{2+}$ spikes in insulin resistance group, the effect of which was abolished by folic acid. These findings suggest that RYR2 leak may trigger spontaneous $Ca^{2+}$ spikes under insulin resistance state while such effect may be ameliorated by folic acid treatment (Fig. 5).

### Assessment of $Ca^{2+}$ handling proteins

To further elucidate the possible role of RYR2 in insulin resistance and/or folic acid-induced myocardial changes, phosphorylation and oxidation of CaMKII were evaluated. Insulin resistance led to an increase in CaMKII phosphorylation, the effect of which was ablated by folic acid. Folic acid itself did not exhibit any effect on CaMKII phosphorylation. Neither insulin resistance nor folic acid exerted any notable effect on oxidation of CaMKII. In addition, neither insulin resistance nor folic acid, or both, affected levels of intracellular $Ca^{2+}$ regulatory proteins SERCA2a and the SERCA inhibitory phospholamban (pan or phosphorylated) (Fig. 6).

## DISCUSSION

The salient data from our present study reveal that insulin resistance using sucrose feeding induces cardiac mechanical defect including echocardiographic, cardiomyocyte contractile, and intracellular $Ca^{2+}$ handling aberrations. In this study, insulin resistance was induced in mice after they reached adulthood, similar to our previous report [23], to mimic the clinical presentations of insulin resistance in adults. In accordance with cardiac mechanical dysfunction, NOS uncoupling was obvious under insulin resistance (decreased NO levels, elevated production of superoxide and $ONOO^-$) along with $Ca^{2+}$ leak from ryanodine receptor. NOS recoupling with folic acid restored NO levels, cardiac contractile and intracellular $Ca^{2+}$ properties as well as suppressed increased levels of superoxide and $ONOO^-$ under insulin resistance. Our data further revealed that insulin resistance promoted CaMKII phosphorylation, the effect of which may be reversed by folic acid. Interestingly, despite the increased superoxide production, little change was noted for the oxidation state of CaMKII. Our findings favored that notion that cardiac dysfunction may be originated from increased $Ca^{2+}$ leak from RYR through CaMKII phosphorylation, which may promote NOS uncoupling in insulin resistance, the effects of which may be alleviated or mitigated by NOS uncoupling using folic acid administration.

Presence of oxidative stress has been well documented in insulin resistance to contribute to detrimental myocardial sequelae [3, 24, 25]. In spite of the rather significant role of ROS in insulin resistance and metabolic syndrome, clinical trials using antioxidants for the management of cardiac diseases have had mixed outcomes, suggesting that targeting ROS producing enzymes may be a better therapeutic option [26]. For example, inhibition of NADPH oxidase (NOX) may prevent NOS uncoupling suggesting a downstream role of NOS uncoupling in NOX-associated ROS production [27]. Interestingly, damage to

mitochondria by oxidative stress causes increased production of superoxide from the damaged mitochondria themselves [28]. Data from our study showed that hearts from insulin resistant mice displayed increased superoxide production. Oxidative stress has been demonstrated to trigger NOS uncoupling rending NOS to produce $O_2^-$ rather than NO [4–6]. This is supported by our current observation of decrease in NO, elevated superoxide and $ONOO^-$ levels under insulin resistance. Four week of folic acid treatment, which is known to recouple NOS [7–9], effectively eliminated NOS-dependent superoxide, restored NO production, suppressed nitrotyrosine formation (depicting $ONOO^-$ levels) and reversed cardiac mechanical dysfunction under insulin resistance, indicating a possible role of NOS recoupling in folic acid-induced beneficial cardiac effect. Although other sources of ROS may exist in our current experimental setting, these data favor that the role of uncoupled NOS as a candidate generator of ROS and subsequently myocardial dysfunction.

Cardiovascular complications in diabetes and insulin resistance often manifest as decreased fractional shortening and impaired cardiomyocyte function [21, 23, 27]. In this study, 8 weeks of sucrose feeding led to a state of insulin resistance and decreased fractional shortening, which were worsened after 12 weeks of sucrose feeding. Due to the contributions of ROS to insulin resistance and the uncoupled state of NOS, we hypothesized that recoupling of NOS may be sufficient to reverse cardiac dysfunction in insulin resistance. With the exception of resting cell length, administration of folic acid restored cardiomyocyte mechanical anomalies and fractional shortening under insulin resistance, supporting a role of NOS uncoupling in insulin resistance-induced cardiac contractile and intracellular $Ca^{2+}$ derangement. Our study noted reduced resting cell length following sucrose feeding length, consistent with the notion of cardiomyocyte atrophy under insulin resistance [29]. It has been suggested that cardiomyocyte atrophy may occur from a loss of insulin/insulin-like growth factor 1 signaling and an increased atrogen-1 expression [30].

It is well conceived that defects in intracellular $Ca^{2+}$ cycling may underscore myocardial contractile dysfunction in insulin resistance [23]. In our hands, high sucrose feeding induced a decreased ΔFFI and prolonged intracellular $Ca^{2+}$ decay rate. Reversal of NOS uncoupling using folic acid restored these parameters to near control levels. Several mechanisms may contribute to the aberrant intracellular $Ca^{2+}$ handling under insulin resistance including redox modification of essential contractile or intracellular $Ca^{2+}$ regulatory proteins [31, 32]. In particular, ryanodine receptor is sensitive to redox activation as well as phosphorylation by CaMKII, both of which alter ryanodine function. Given that impaired RYR2 function has been documented in diabetic heart complications [33], RYR2 $Ca^{2+}$ leak was evaluated in this study. Analysis of tetracaine-dependent resting intracellular $Ca^{2+}$ rise revealed that insulin resistance displays a significant $Ca^{2+}$ leak through the RYR receptor to trigger spontaneous cardiomyocyte contraction.

To better understand intracellular $Ca^{2+}$ cycling defects under insulin resistance, other proteins essential for intracellular $Ca^{2+}$ homeostasis were evaluated including SERCA2a, phospholamban and CaMKII given the pivotal roles of these proteins in intracellular $Ca^{2+}$ handling [13]. CaMKII is considered a master regulator for intracellular $Ca^{2+}$ cycling through its phosphorylation of RYR and phospholamban to govern their respective activity [34]. Considering defective RYR channel function observed in our study, it is plausible to speculate the role of CaMKII as a likely target for NOS uncoupling in insulin resistance. Both oxidation and phosphorylation of CaMKII were evaluated as both play a key role in its enzymatic activation [35]. Interestingly, little effect was noted in oxidation of CaMKII somewhat inconsistent with enhanced superoxide production following sucrose feeding. To the contrary, phosphorylation of CaMKII was increased under insulin resistance, the effect of which was reversed by folic acid. These data strongly suggest that CaMKII is a directly

downstream target for NOS uncoupling to underlie cardiac contractile dysfunction in insulin resistance.

In summary, our findings indicated that NOS uncoupling may be the underlying mechanism responsible for cardiac dysfunction in insulin resistance. Our data revealed that insulin resistance promoted NOS uncoupling leading to echocardiographic and cardiomyocyte abnormalities in conjunction with intracellular $Ca^{2+}$ dysregulation. Underlying this contractile dysfunction is impaired function of the RYR $Ca^{2+}$ channel leading to resting $Ca^{2+}$ leak, which can be attributed to phosphorylation of CaMKII. Perhaps the most significant finding from our study is that the common dietary supplement folic acid effectively restores proper NOS function and eliminates cardiac abnormalities under insulin resistance, suggesting the therapeutic promises of NOS recoupling in insulin resistance-induced cardiac anomalies. The beneficial effect of folic acid on cardiac anomalies in insulin resistance is consistent with that offered by the antioxidant metallothionein and catalase [23, 36], which are known to alleviate oxidative stress and preserve NOS coupling [6].

## Supplementary Material

Refer to Web version on PubMed Central for supplementary material.

## Acknowledgments

This work was supported in part by the NIH P20 GM134012.

## BIBLIOGRAPHY

1. Go AS, Mozaffarian D, Roger VL, Benjamin EJ, Berry JD, Borden WB, Bravata DM, Dai S, Ford ES, Fox CS, Franco S, Fullerton HJ, Gillespie C, Hailpern SM, Heit JA, Howard VJ, Huffman MD, Kissela BM, Kittner SJ, Lackland DT, Lichtman JH, Lisabeth LD, Magid D, Marcus GM, Marelli A, Matchar DB, McGuire DK, Mohler ER, Moy CS, Mussolino ME, Nichol G, Paynter NP, Schreiner PJ, Sorlie PD, Stein J, Turan TN, Virani SS, Wong ND, Woo D, Turner MB. American Heart Association Statistics, C; Stroke Statistics, S. Executive summary: heart disease and stroke statistics-2013 update: a report from the American Heart Association. Circulation. 2013; 127:143–152. [PubMed: 23283859]
2. Mellor KM, Ritchie RH, Delbridge LM. Reactive oxygen species and insulin-resistant cardiomyopathy. Clin Exp Pharmacol Physiol. 2010; 37:222–228. [PubMed: 19671065]
3. Tsutsui H, Kinugawa S, Matsushima S. Oxidative stress and heart failure. Am J Physiol Heart Circ Physiol. 2011; 301:H2181–H2190. [PubMed: 21949114]
4. Roe ND, Ren J. Nitric oxide synthase uncoupling: A therapeutic target in cardiovascular diseases. Vascul Pharmacol. 2012
5. Moens AL, Takimoto E, Tocchetti CG, Chakir K, Bedja D, Cormaci G, Ketner EA, Majmudar M, Gabrielson K, Halushka MK, Mitchell JB, Biswal S, Channon KM, Wolin MS, Alp NJ, Paolocci N, Champion HC, Kass DA. Reversal of cardiac hypertrophy and fibrosis from pressure overload by tetrahydrobiopterin: efficacy of recoupling nitric oxide synthase as a therapeutic strategy. Circulation. 2008; 117:2626–2636. [PubMed: 18474817]
6. Ceylan-Isik AF, Guo KK, Carlson EC, Privratsky JR, Liao SJ, Cai L, Chen AF, Ren J. Metallothionein abrogates GTP cyclohydrolase I inhibition-induced cardiac contractile and morphological defects: role of mitochondrial biogenesis. Hypertension. 2009; 53:1023–1031. [PubMed: 19398661]
7. Moens AL, Champion HC, Claeys MJ, Tavazzi B, Kaminski PM, Wolin MS, Borgonjon DJ, Van Nassauw L, Haile A, Zviman M, Bedja D, Wuyts FL, Elsaesser RS, Cos P, Gabrielson KL, Lazzarino G, Paolocci N, Timmermans JP, Vrints CJ, Kass DA. High-dose folic acid pretreatment blunts cardiac dysfunction during ischemia coupled to maintenance of high-energy phosphates and reduces postreperfusion injury. Circulation. 2008; 117:1810–1819. [PubMed: 18362233]

8. Gao L, Siu KL, Chalupsky K, Nguyen A, Chen P, Weintraub NL, Galis Z, Cai H. Role of uncoupled endothelial nitric oxide synthase in abdominal aortic aneurysm formation: treatment with folic acid. Hypertension. 2012; 59:158–166. [PubMed: 22083158]
9. Gao L, Chalupsky K, Stefani E, Cai H. Mechanistic insights into folic aciddependent vascular protection: dihydrofolate reductase (DHFR)-mediated reduction in oxidant stress in endothelial cells and angiotensin II-infused mice: a novel HPLC-based fluorescent assay for DHFR activity. J Mol Cell Cardiol. 2009; 47:752–760. [PubMed: 19660467]
10. Mishra PK, Givvimani S, Metreveli N, Tyagi SC. Attenuation of beta2-adrenergic receptors and homocysteine metabolic enzymes cause diabetic cardiomyopathy. Biochem Biophys Res Commun. 2010; 401:175–181. [PubMed: 20836991]
11. Kolling J, Scherer EB, da Cunha AA, da Cunha MJ, Wyse AT. Homocysteine induces oxidative-nitrative stress in heart of rats: prevention by folic acid. Cardiovasc Toxicol. 2011; 11:67–73. [PubMed: 21076891]
12. Moens AL, Vrints CJ, Claeys MJ, Timmermans JP, Champion HC, Kass DA. Mechanisms and potential therapeutic targets for folic acid in cardiovascular disease. Am J Physiol Heart Circ Physiol. 2008; 294:H1971–H1977. [PubMed: 18375715]
13. Hadri L, Hajjar RJ. Calcium cycling proteins and their association with heart failure. Clin Pharmacol Ther. 2011; 90:620–624. [PubMed: 21832991]
14. Ochi R, Gupte SA. Ryanodine receptor: a novel therapeutic target in heart disease. Recent Pat Cardiovasc Drug Discov. 2007; 2:110–118. [PubMed: 18221109]
15. Currie S, Elliott EB, Smith GL, Loughrey CM. Two candidates at the heart of dysfunction: The ryanodine receptor and calcium/calmodulin protein kinase II as potential targets for therapeutic intervention-An in vivo perspective. Pharmacol Ther. 2011; 131:204–220. [PubMed: 21414358]
16. Shao CH, Wehrens XH, Wyatt TA, Parbhu S, Rozanski GJ, Patel KP, Bidasee KR. Exercise training during diabetes attenuates cardiac ryanodine receptor dysregulation. J Appl Physiol. 2009; 106:1280–1292. [PubMed: 19131475]
17. Alkaitis MS, Crabtree MJ. Recoupling the cardiac nitric oxide synthases: tetrahydrobiopterin synthesis and recycling. Current heart failure reports. 2012; 9:200–210. [PubMed: 22711313]
18. Dong F, Kandadi MR, Ren J, Sreejayan N. Chromium (D-phenylalanine)3 supplementation alters glucose disposal, insulin signaling, and glucose transporter-4 membrane translocation in insulin-resistant mice. J Nutr. 2008; 138:1846–1851. [PubMed: 18806091]
19. Shannon TR, Ginsburg KS, Bers DM. Quantitative assessment of the SR Ca2+ leak-load relationship. Circ Res. 2002; 91:594–600. [PubMed: 12364387]
20. Gonzalez DR, Treuer AV, Castellanos J, Dulce RA, Hare JM. Impaired S-nitrosylation of the ryanodine receptor caused by xanthine oxidase activity contributes to calcium leak in heart failure. J Biol Chem. 2010; 285:28938–28945. [PubMed: 20643651]
21. Ren J, Duan J, Thomas DP, Yang X, Sreejayan N, Sowers JR, Leri A, Kajstura J, Gao F, Anversa P. IGF-I alleviates diabetes-induced RhoA activation, eNOS uncoupling, and myocardial dysfunction. American journal of physiology. Regulatory, integrative and comparative physiology. 2008; 294:R793–R802.
22. Dong F, Zhang X, Culver B, Chew HG Jr, Kelley RO, Ren J. Dietary iron deficiency induces ventricular dilation, mitochondrial ultrastructural aberrations and cytochrome c release: involvement of nitric oxide synthase and protein tyrosine nitration. Clin Sci (Lond). 2005; 109:277–286. [PubMed: 15877545]
23. Dong F, Fang CX, Yang X, Zhang X, Lopez FL, Ren J. Cardiac overexpression of catalase rescues cardiac contractile dysfunction induced by insulin resistance: Role of oxidative stress, protein carbonyl formation and insulin sensitivity. Diabetologia. 2006; 49:1421–1433. [PubMed: 16586065]
24. Giacco F, Brownlee M. Oxidative stress and diabetic complications. Circ Res. 2010; 107:1058–1070. [PubMed: 21030723]
25. Murarka S, Movahed MR. Diabetic cardiomyopathy. J Card Fail. 2010; 16:971–979. [PubMed: 21111987]
26. Sheikh-Ali M, Chehade JM, Mooradian AD. The antioxidant paradox in diabetes mellitus. Am J Ther. 2011; 18:266–278. [PubMed: 19797943]

27. Roe ND, Thomas DP, Ren J. Inhibition of NADPH oxidase alleviates experimental diabetes-induced myocardial contractile dysfunction. Diabetes Obes Metab. 2011; 13:465–473. [PubMed: 21272185]

28. Van Remmen H, Richardson A. Oxidative damage to mitochondria and aging. Exp Gerontol. 2001; 36:957–968. [PubMed: 11404044]

29. Roe ND, Ren J. Akt2 knockout mitigates chronic iNOS inhibition-induced cardiomyocyte atrophy and contractile dysfunction despite persistent insulin resistance. Toxicol Lett. 2011; 207:222–231. [PubMed: 21964073]

30. Wang H, Liu D, Cao P, Lecker S, Hu Z. Atrogin-1 affects muscle protein synthesis and degradation when energy metabolism is impaired by the antidiabetes drug berberine. Diabetes. 2010; 59:1879–1889. [PubMed: 20522589]

31. Bogeski I, Kappl R, Kummerow C, Gulaboski R, Hoth M, Niemeyer BA. Redox regulation of calcium ion channels: chemical and physiological aspects. Cell Calcium. 2011; 50:407–423. [PubMed: 21930299]

32. Sumandea MP, Steinberg SF. Redox signaling and cardiac sarcomeres. J Biol Chem. 2011; 286:9921–9927. [PubMed: 21257753]

33. Turan B, Vassort G. Ryanodine receptor: a new therapeutic target to control diabetic cardiomyopathy. Antioxid Redox Signal. 2011; 15:1847–1861. [PubMed: 21091075]

34. Anderson ME, Brown JH, Bers DM. CaMKII in myocardial hypertrophy and heart failure. J Mol Cell Cardiol. 2011; 51:468–473. [PubMed: 21276796]

35. Erickson JR, He BJ, Grumbach IM, Anderson ME. CaMKII in the cardiovascular system: sensing redox states. Physiol Rev. 2011; 91:889–915. [PubMed: 21742790]

36. Fang CX, Dong F, Ren BH, Epstein PN, Ren J. Metallothionein alleviates cardiac contractile dysfunction induced by insulin resistance: role of Akt phosphorylation, PTB1B, PPARgamma and c-Jun. Diabetologia. 2005; 48:2412–2421. [PubMed: 16172869]

## Research highlights

- We examined the effect of folic acid on insulin resistance-induced heart dysfunction;
- Folic acid rescues against insulin resistance-induced cardiac dysfunction;
- The beneficial effect of folic acid was related to improved intracellular $Ca^{2+}$ handling;

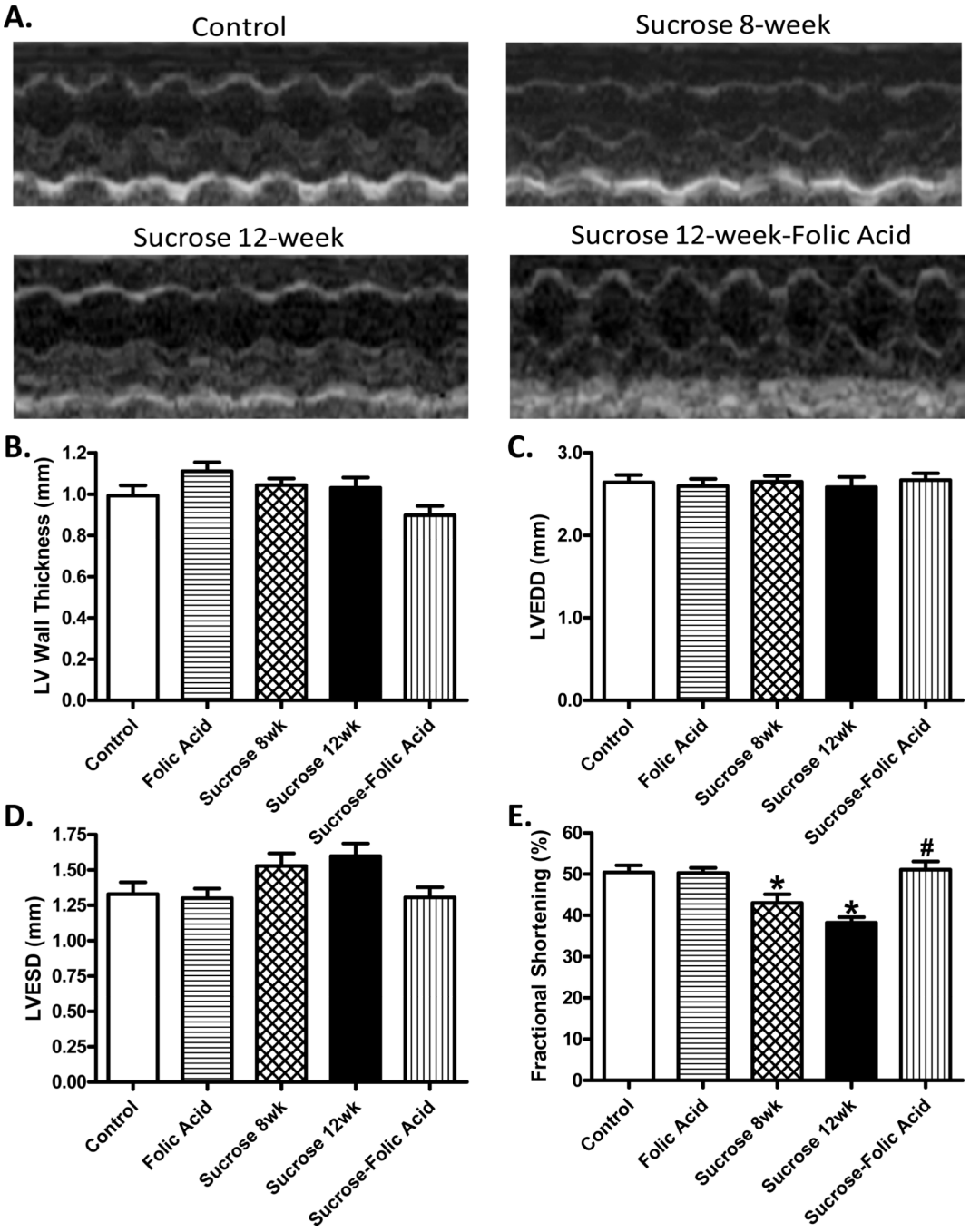


**Fig. 1.**

Effect of insulin resistance (sucrose feeding for 8 or 12 weeks) and folic acid treatment on echocardiographic properties. A: Representative echocardiographic images from defined groups; B: Left ventricular (LV) wall thickness; C: LV end diastolic diameter (LVEDD); D: LV end systolic diameter (LVESD); and E: Fractional shortening. Mean ± SEM, n = 7–22 mice per group, *$p < 0.05$ *vs.* Control, #$p < 0.05$ *vs.* Sucrose group.

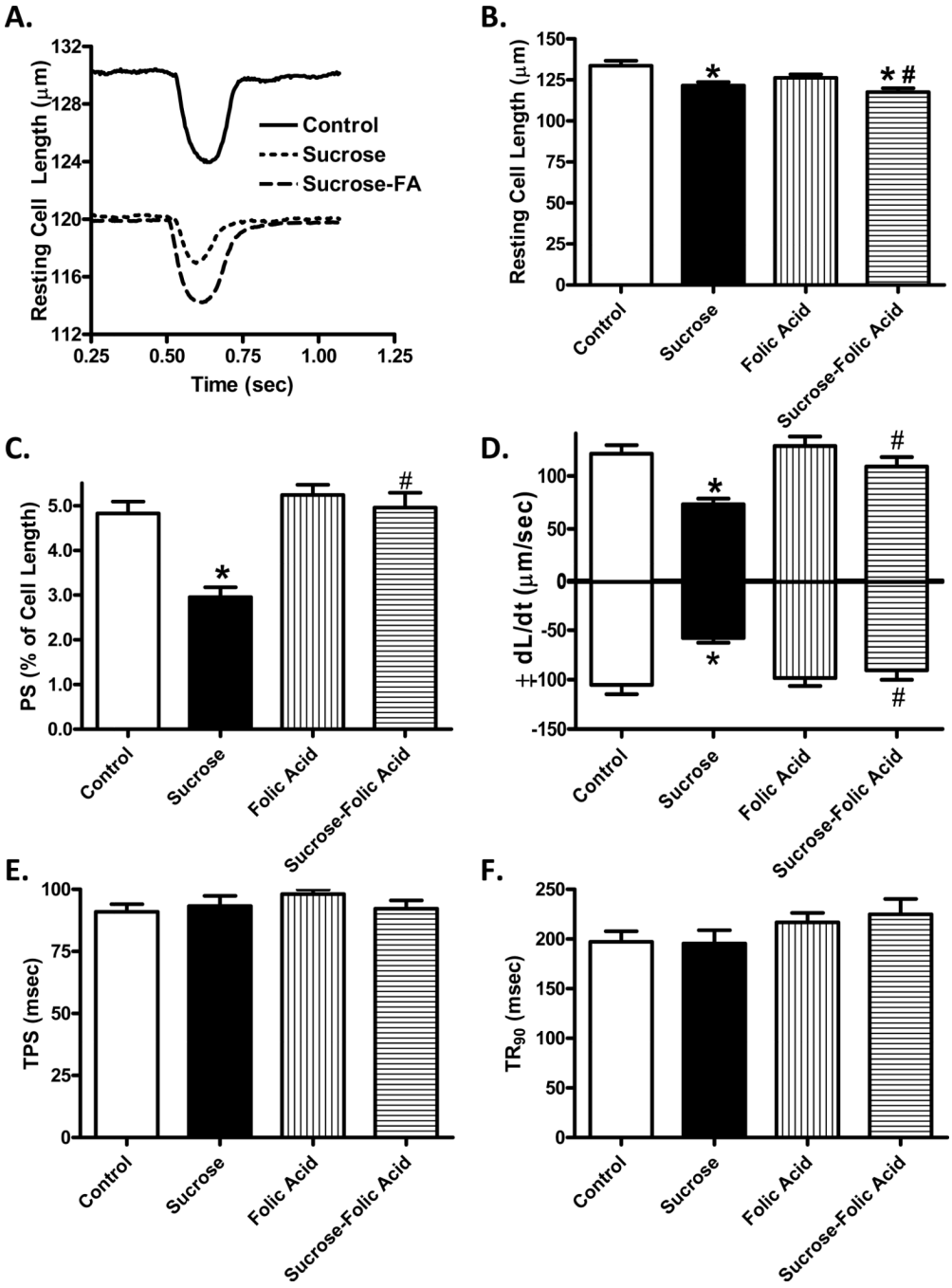


**Fig. 2.**

Effect of folic acid treatment on insulin resistance-induced changes in cardiomyocyte contractile properties. A: Representative cell shortening traces; B: Resting cell length; C: Peak shortening amplitude (normalized to resting cell length); D: Maximum velocity of shortening/relengthening (± dL/dt); E: Time-to-peak shortening (TPS); and F: Time-to-peak relengthening ($TR_{90}$). Mean ± SEM, n= 109–165 cells from 3 mice per group, *$p < 0.05$ *vs.* Control, #$p < 0.05$ *vs.* Sucrose group.

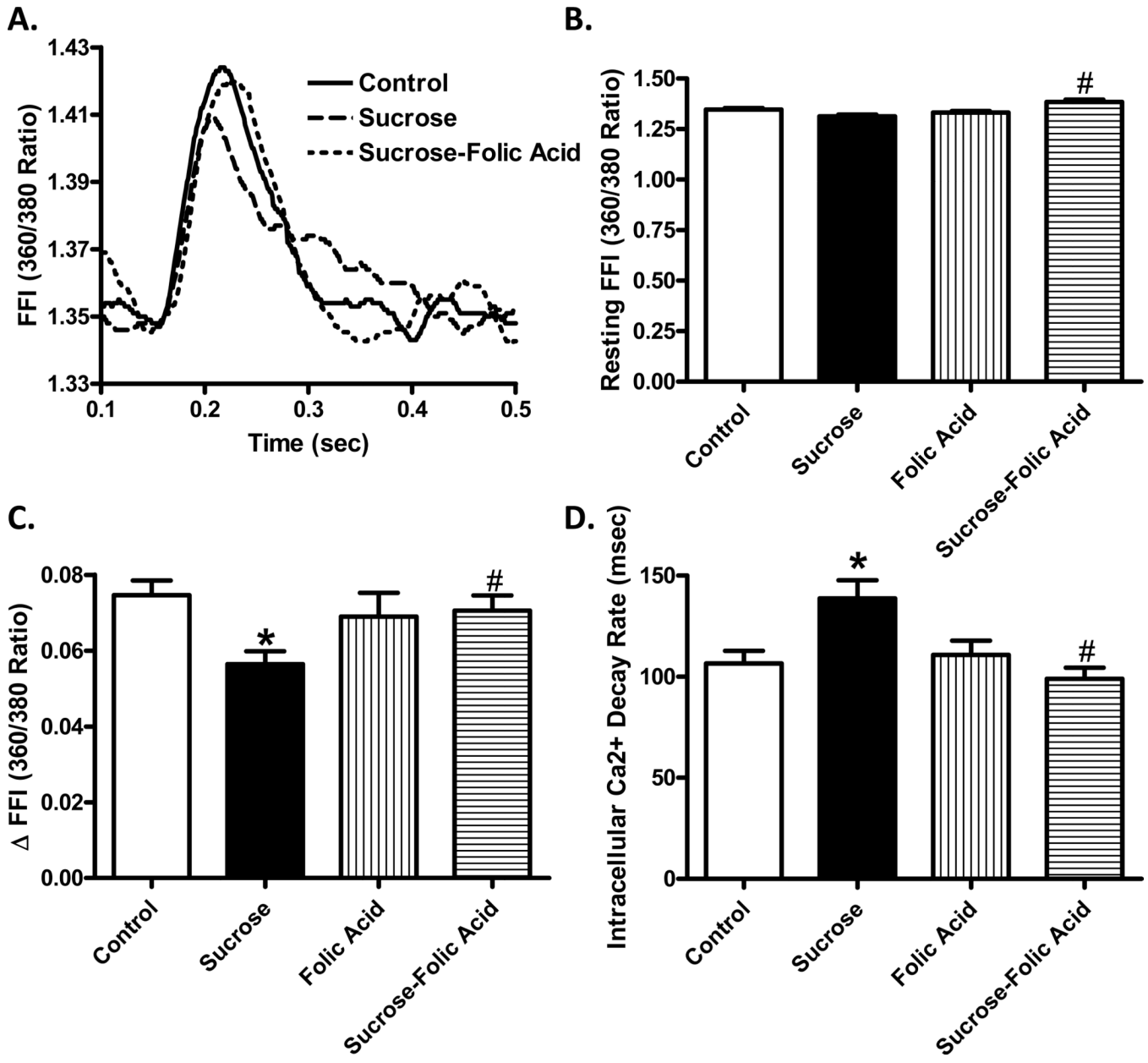


**Fig. 3.**

Effect of NOS recoupling using folic acid on insulin resistance-induced intracellular $Ca^{2+}$ handling. A: Representative intracellular $Ca^{2+}$ traces from control and sucrose groups with or without folic acid treatment; B: Resting fura-2 fluorescence intensity (FFI); C: Electronically-stimulated rise in FFI (ΔFFI); and D: Intracellular $Ca^{2+}$ decay rate. Mean ± SEM, n = 99 – 111 cells from 3 mice per group, *p < 0.05 *vs.* Control, #p < 0.05 *vs.* Sucrose group.

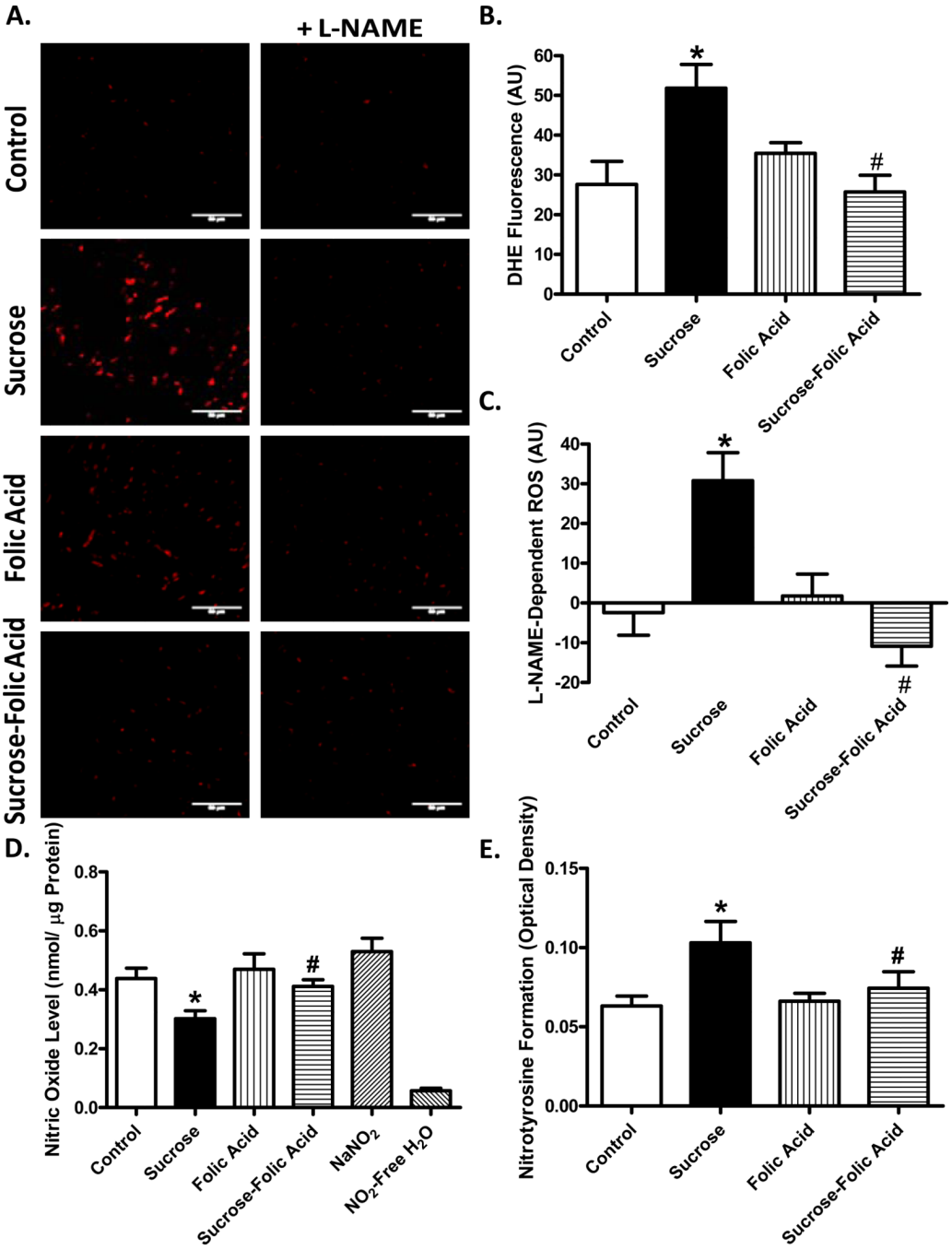


**Fig. 4.**

Effect of folic acid on superoxide production, NOS uncoupling, NO and $ONOO^-$ levels in insulin resistance. A: Representative images of DHE-stained heart sections incubated with or without L-NAME (1 mM); B: Pooled data summarizing DHE fluorescence intensity; C: L-NAME-dependent ROS production in each group; D: Cardiomyocyte NO levels ($NaNO_2$ and $NO_2$-free $H_2O$ used as positive and negative controls, respectively); and E: Myocardial ONOOlevels measured by nitrotyrosine formation. Mean ± SEM, n = 3 hearts per group, *p < 0.05 *vs.* Control, #p < 0.05 *vs.* Sucrose group.

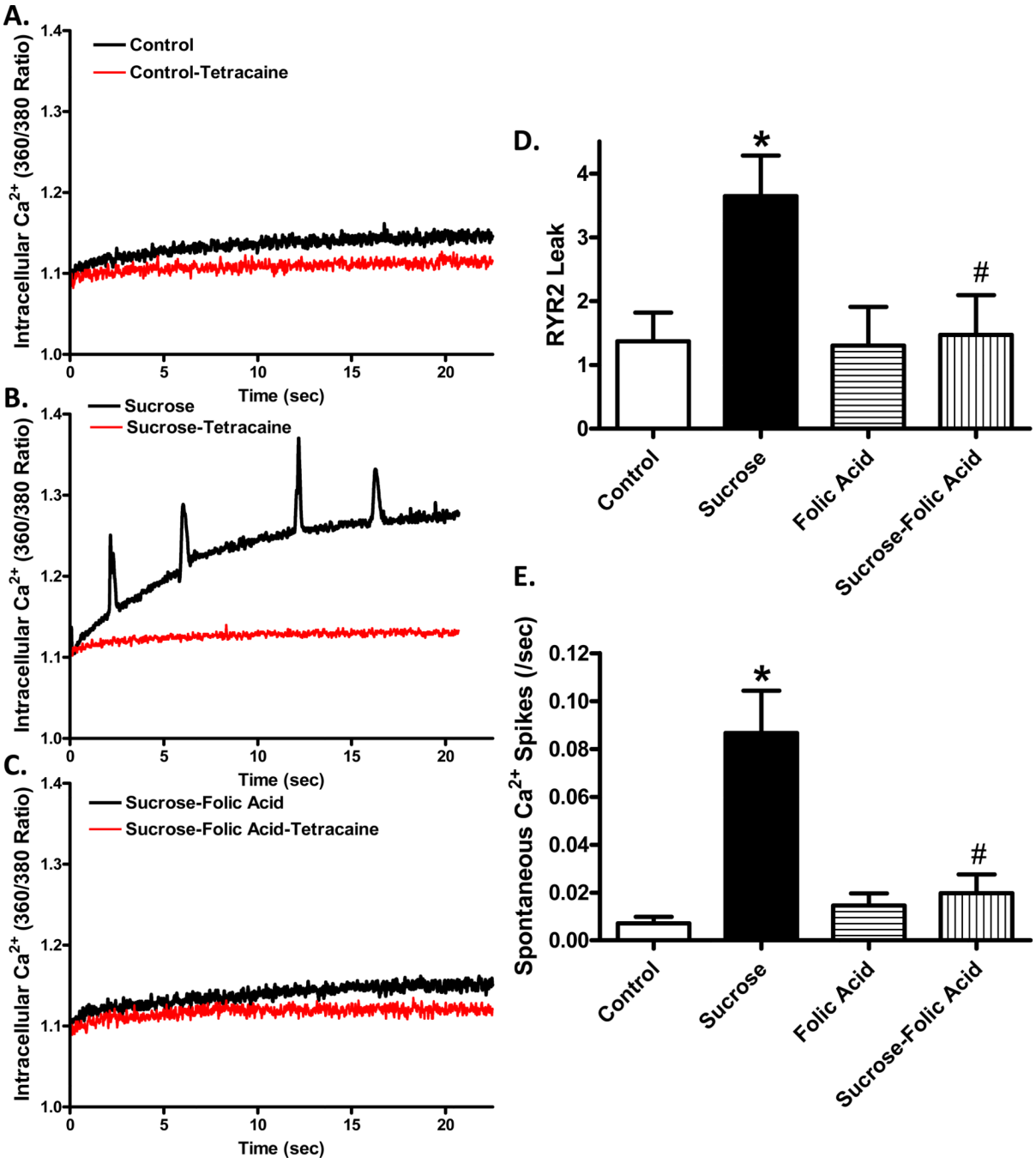


**Fig. 5.**

Role of NOS uncoupling on insulin resistance-induced $Ca^{2+}$ leak. Cardiomyocytes from control or sucrose-fed mice with or without folic acid treatment were assessed for intracellular $Ca^{2+}$ levels for 80 seconds in the presence of a $0Na^{+}$-$0Ca^{2+}$ buffer. A: Representative traces from control and insulin resistant murine cardiomyocytes with and without the RYR inhibitor tetracaine (1 mM); B: Diastolic $Ca^{2+}$ leak as calculated by the difference in AUC between $0Na^{+}$-$0Ca^{2+}$ and $0Na^{+}$-$0Ca^{2+}$+tetracaine; C: Number of spontaneous contraction. Mean ± SEM, n = 18 – 30 cells from 3 mice per group, *$p < 0.05$ *vs.* Control, #$p < 0.05$ *vs.* Sucrose group.

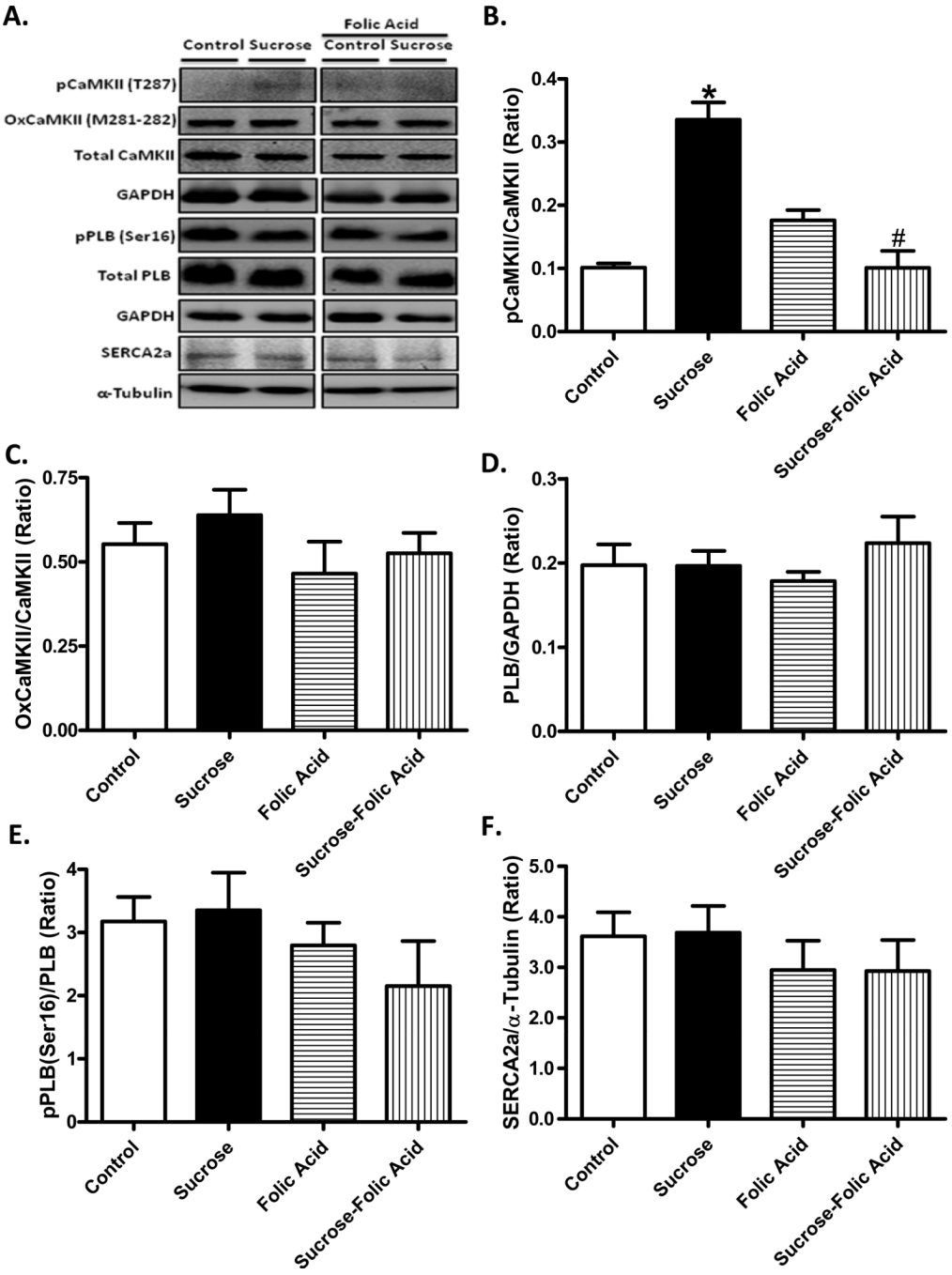


**Fig. 6.**

Effect of insulin resistance and folic acid treatment on CaMKII and intracellular $Ca^{2+}$ regulatory proteins. A: Representative gel blots depicting levels of phosphorylated, oxidized and total CaMKII, total and phosphorylated phospholamban (PLB) and SERCA2a using specific antibodies (GAPDH as loading controls); B: Phosphorylated CaMKII (pCaMKII, $Thr^{287}$); C: Oxidized CaMKII ($Met^{281–282}$); D: PLB expression; E: Phosphorylated PLB ($Ser^{16}$)-to-PLB ratio; and F: SERCA2a expression. Mean ± SEM, n = 4–5 hearts per group, *$p < 0.05$ *vs.* Control, #$p < 0.05$ *vs.* Sucrose group.

## Table 1

Biometric properties of control and sucrose-fed mice treated with or without folic acid (15 mg/kg/day in drinking water for 4 weeks)

| | Control | Sucrose | Folic Acid | Sucrose-Folic Acid |
|---|---|---|---|---|
| Body Weight (g) | 30.0 ± 0.9 | 28.1 ± 1.9 | 31.2 ± 1.8 | 27.6 ± 0.9 |
| Heart Weight (mg) | 162 ± 13 | 152 ± 14 | 169 ± 11 | 137 ± 2 |
| HW/TL (mg/mm) | 8.7 ± 0.6 | 8.1 ± 0.6 | 9.2 ± 0.6 | 7.4 ± 0.1 |
| Liver Weight (g) | 1.77 ± 0.08 | 1.54 ± 0.13 | 1.67 ± 0.11 | 1.48 ± 0.08 |
| LW/TL (g/mm) | 0.095 ± 0.003 | 0.082 ± 0.006 | 0.091 ± 0.006 | 0.080 ± 0.004 |
| Kidney Weight (mg) | 475 ± 11 | 471 ± 46 | 497 ± 12 | 412 ± 18 |
| KW/TL (mg/mm) | 25.6 ± 1.0 | 25.1 ± 2.1 | 27.0 ± 0.6 | 22.2 ± 1.1 |
| Tibia Length (mm) | 18.6 ± 0.5 | 18.7 ± 0.3 | 18.4 ± 0.1 | 18.6 ± 0.4 |

HW = heart weight; LW = liver weight; KW = kidney weight; TL = tibial length, Mean ± SEM, n = 4–5 mice per group, $p > 0.05$ among any groups.